Refined solution structure of a liganded type 2 wheat nonspecific lipid transfer protein

Jean-Luc Pons, Frédéric de Lamotte, Marie Francoise M. F. Gautier, Marc-André Delsuc

THE JOURNAL OF BIOLOGICAL CHEMISTRY
Vol. 278, No. 16, Issue of April 18, pp. 14249–14256, 2003

Printed in U.S.A.

Refined Solution Structure of a Liganded Type 2 Wheat Nonspecific Lipid Transfer Protein*

Received for publication, November 15, 2002, and in revised form, January 10, 2003
Published, JBC Papers in Press, January 13, 2003, DOI 10.1074/jbc.M211683200

Jean-Luc Pons‡, Frédéric de Lamotte§, Marie-Françoise Gautier§, and Marc-André Delsuc‡¶

From the ‡Centre de Biochimie Structurale, INSERM, CNRS, Université Montpellier I, 15 Ave C. Flahault, 34 060 Montpellier, France and §Unité Mixte de Recherche Génomique Appliquée aux Caractères Agronomique, INRA, 2 Place Viala, 34 060 Montpellier, cedex 01, France

The refined structure of a wheat type 2 nonspecific lipid transfer protein (ns-LTP2) liganded with L-α-palmitoylphosphatidylglycerol has been determined by NMR. The ^{15}N-labeled protein was produced in *Pichia pastoris*. Physicochemical conditions and ligandation were intensively screened to obtain the best NMR spectra quality. This ns-LTP2 is a 67-residue globular protein with a diameter of about 30 Å. The structure is composed of five helices forming a right superhelix. The protein presents an inner cavity, which has been measured at 341 Å^3. All of the helices display hydrophobic side chains oriented toward the cavity. The phospholipid is found in this cavity. Its fatty acid chain is completely inserted in the protein, the L-α-palmitoylphosphatidylglycerol glycerol moiety being located on a positively charged pocket on the surface of the protein. The superhelix structure of the protein is coiled around the fatty acid chain. The overall structure shows similarities with ns-LTP1. Nevertheless, large three-dimensional structural discrepancies are observed for the H3 and H4 α-helices, the C-terminal region, and the last turn of the H2 helix. The lipid is orthogonal to the orientation observed in ns-LTP1. The volume of the hydrophobic cavity appears to be in the same range as the one of ns-LTP1, despite the fact that ns-LTP2 is shorter by 24 residues.

Plant nonspecific lipid transfer proteins (ns-LTPs)[1] were first isolated from spinach leaves and named based on their ability to mediate *in vitro* the transfer of phospholipids between membranes (1). ns-LTPs are widely distributed and form a superfamily of related proteins subdivided into two families: the type 1 ns-LTPs (ns-LTP1) and the type 2 ns-LTPs (ns-LTP2) (see Refs. 2 and 3 for review). Both families are multigenic, and more than 150 sequences of plant ns-LTPs are listed in data bases. Only a limited number of proteins have been isolated from plant, and *in vitro* lipid transfer or binding has been demonstrated for an even more limited number of proteins.

The biological functions of ns-LTP1 have not yet been clearly determined, the most favored hypothesis being a role in the transport of cutin monomers (4, 5) or in plant defense mechanisms (6–8) for ns-LTP1. ns-LTP2 gene expression has been reported in the *Zinnia elegans* cell differentiation process (9, 10), in barley and rice developing seeds (11, 12), under abiotic stress conditions in barley roots (12), or during nodulation in *Vigna unguiculata* root hairs (13). However, there is no biological evidence of their function in these different contexts. The recent discovery that some ns-LTPs are pan-allergens of plant-derived foods has brought new interest for their study. Most of the ns-LTP allergens identified so far belong to the ns-LTP1 family (14–17), whereas ns-LTP2 has been reported only as a potent allergen of the pollen of *Brassica rapa* (18).

The three-dimensional structure of four cereal ns-LTP1s has been determined, *i.e.* wheat (19), barley (20), maize (21, 22), and rice (23, 24). In addition, seven structures of plant ns-LTP1 in complex with ligands have been determined, including those of maize ns-LTP1 with palmitate (21) or palmitoyl-lyso-phosphatidylcholine (22), barley ns-LTP1 with palmitoyl CoA (25) or palmitate (26), and wheat ns-LTP1 with di-myristoyl-phosphatidylglycerol (27), lyso-myristoyl-phosphatidylcholine (28), or prostaglandin B2 (29). All of these data showed that ns-LTP1 are compact single domain proteins whose fold is stabilized by four disulfide bonds. They are characterized by a four-α-helix bundle and a C-terminal region with no regular secondary structure. The most interesting feature of ns-LTP1 structure is the tunnel-like hydrophobic cavity that runs through the molecule and appears as a potential site for lipid binding. Although plant ns-LTP1s exhibit very similar global folds, the shape and size of this hydrophobic cavity vary considerably depending on the protein and/or on the ligand. This clearly indicates a high plasticity of the cavity that is able to accommodate a variety of hydrophobic molecules. In contrast, an antifungal protein extracted from onion seeds that showed a structure similar to those of ns-LTP1 except that the internal cavity, obstructed by several aromatic side chains, is unable to transfer lipids (30).

ns-LTP1s have been studied more extensively than ns-LTP2s that are distinct in terms of primary sequence with less than 30% homology (Fig. 1), size (7 kDa *versus* 9 kDa), and lipid transfer efficiency. In wheat, both ns-LTP1 and ns-LTP2 have been biochemically characterized, and ns-LTP2 exhibits a higher lipid transfer activity than ns-LTP1 (31). They share the same 8-cysteine skeleton, but their disulfide bond assignment has been shown to be different (32). Because the wheat ns-LTP2 exhibits a lipid transfer activity, one can hypothesize the presence of an hydrophobic cavity. However, whether ns-LTP2s have a fold that is similar to or different from that of ns-LTP1

* The costs of publication of this article were defrayed in part by the payment of page charges. This article must therefore be hereby marked "*advertisement*" in accordance with 18 U.S.C. Section 1734 solely to indicate this fact.

The atomic coordinates and structure factors (code 1N89) have been deposited in the Protein Data Bank, Research Collaboratory for Structural Bioinformatics, Rutgers University, New Brunswick, NJ (http://www.rcsb.org/).

¶ To whom correspondence should be addressed. Fax: 33-467-52-96-23; E-mail: MA.Delsuc@cbs.cnrs.fr.

[1] The abbreviations used are: ns-LTP, nonspecific lipid transfer protein; LPG, L-α-palmitoylphosphatidylglycerol; HSQC, heteronuclear single-quantum spectroscopy; NOE, nuclear Overhauser effect; NOESY, NOE-edited spectroscopy; TOCSY, total correlation spectroscopy; COSY, correlation spectroscopy; MALDI-TOF, matrix-assisted laser desorption/ionization-time of flight.

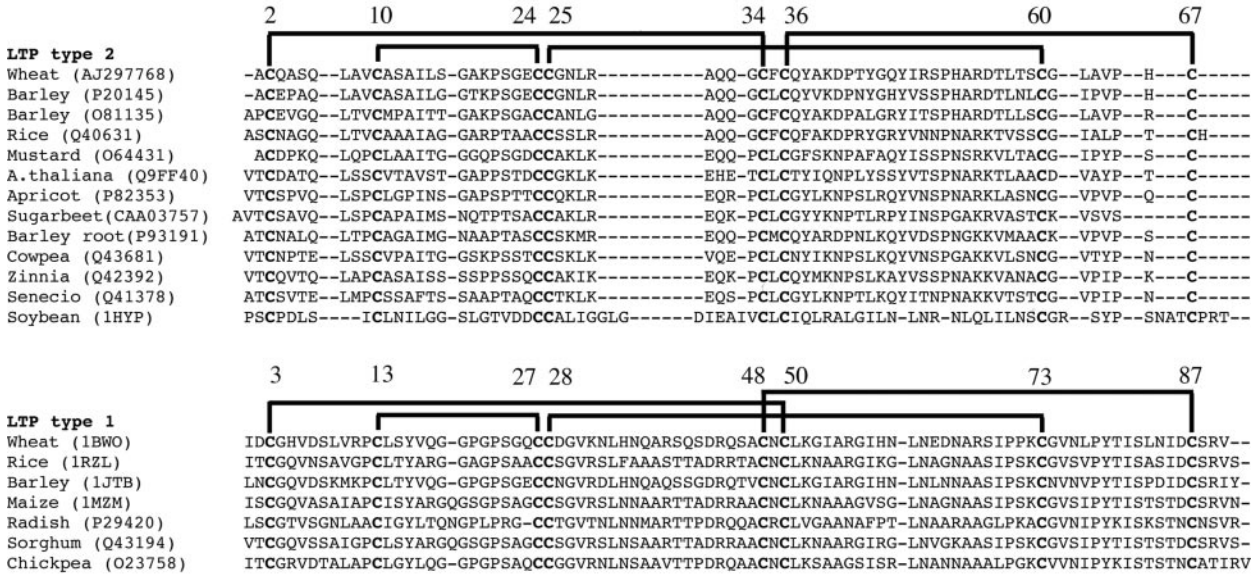

FIG. 1. **Primary sequence alignment of various ns-LTP1 and ns-LTP2.** The proteins are detailed by the Swiss-Prot accession number or the Protein Data Bank accession number when available. The disulfide bridges are shown with *black lines* and numbered according to wheat ns-LTPs.

remained to be elucidated at the initiation of the present work. This paper presents the refined solution structure of a recombinant wheat ns-LTP2 liganded with a C16 lyso-phospholipid. In the final stages of preparation of this manuscript, the structure of a rice ns-LTP2 was reported (33) (Protein Data Bank entry 1L6H).

EXPERIMENTAL PROCEDURES

Production/Purification—The *Pichia pastoris* transformant GS115-Tdltp18-tr5.2 (34) expressing a wheat ns-LTP2 was used for the production of the ^{15}N-labeled protein. Production was carried out in an Applikon fermentor (400 ml of culture) with 99.4% ^{15}N-labeled ammonium sulfate (Eurisotop) as nitrogen source. Labeled $(^{15}NH_4)_2SO_2$ (0.9% w/v) was added from the very beginning of the biomass production phase and during the induction phase at 0, 24, and 48 h (0.27, 0.27, and 0.36 w/v, respectively). Production of ns-LTP2 was induced by methanol after 22 h of culture and lasted for 77 h. The amount of secreted protein was estimated by densitometer analysis of SDS gels, using purified ns-LTP2 as a standard. Folding and accumulation of the recombinant protein was also directly monitored by ^{15}N HSQC NMR (34). A nonlabeled sample was also produced as described earlier (35).

The protein was purified from culture supernatant by a single-step procedure (36) using expanded bed chromatography (Streamline SP-XL; Amersham Biosciences), and 650 mg of protein were obtained. The column was equilibrated in 30 mM sodium acetate, pH 5.5, and the proteins were eluted with 1 M NaCl. The purified protein was dialyzed against H_2O, lyophilized, and analyzed by SDS-PAGE, MALDI-TOF, and HSQC. MALDI-TOF mass spectrometry experiments were conducted on BiFlex III mass spectrometer (Bruker Daltonics, Bremen, Germany). 100 pmol of the protein were solubilized in 10 μl of water containing 0.1% trifluoroacetic acid. A 0.5-μl sample of this solution was mixed with 0.5 μl of matrix (a saturated solution of α-cyano-4-hydroxycinnamic acid in water/acetonitrile 50/50 v/v) and deposited on the target (dried droplet preparation). The spectra were recorded on the linear positive mode using the Pulsed Ion Extraction. For the tryptic digestion analysis, the protein was reduced by dithiothreitol and alkylated by iodoacetamide prior to digestion. The protein was digested for 4 h by trypsin (modified, sequencing grade from Roche Molecular Biochemicals) in 25 mM ammonium carbonate buffer (pH 8) at an enzyme/protein ratio of 1/20 (w/w). Proteolysis was stopped by adding diluted trifluoroacetic acid. The digest mixture was analyzed by MALDI-TOF mass spectrometry in the positive reflector mode.

Mass spectrometry analysis revealed the heterogeneity of the purified protein, 15% being glycosylated. The sugar moiety, assumed to be mannose, were located in the first 29-residue fragment. The protein was thus further purified using reverse phase chromatography (Source 15 RPC/Akta Purifier 10; Amersham Biosciences), for a final amount of 300 mg of protein.

NMR and Fluorescence ns-LTP2/Lipid Screening—Preliminary experiments revealed that NMR spectra could be significantly improved when ns-LTP2 interacts with a lipid. To find the best conditions for the study, several ligands and physicochemical conditions were screened by fluorimetry as well as by NMR. The interaction with L-α-palmitoylphosphatidylglycerol (LPG), L-α-palmitoylphosphatidylcholine, dimyristoylphosphatidylglycerol, dimyristoylphosphatidylcholine, and cholesterol was tested by fluorimetry and NMR. Lipids from Avanti polar were prepared in solution in ethanol at a concentration of 10 mM or in small unilamellar vesicle obtained by sonication in H_2O.

The fluorescence experiments were performed on a ISS instrument equipped with Hamatsu detector at 294 K in a 150-μl volume, excitation was set at 275 nm (300 W), and the spectra were recorded between 285 and 400 nm. Increasing amounts of ligand (0.1–100 equivalent) were added to a solution of ns-LTP2 (30 μM).

NOESY spectra were recorded for 12 h on a Bruker 600 MHz spectrometer at 300 K on a 2.7 mM ns-LTP2 solution in 60 mM phosphate buffer containing 1 eq of lipid. HSQC spectra were recorded for 30 min on a Bruker 400 MHz on a 1.1 mM ns-LTP2 solution, 10% D_2O. The impact of several parameters was investigated: temperature (300–315 K), pH (3.45–6.5), ionic strength (0–100 mM NaCl and 0–60 mM phosphate buffer), and lipid concentration (0–1.5 eq).

Sequence Alignment and Model Prediction—Primary sequence alignments were performed with the following software: CLUSTAL W (37) and Psi-Blast (38). Early three-dimensional models of construction and three-dimensional comparison were performed using a web metaserver (bioserv.cbs.cnrs.fr; Ref. 39) with the following threading methods: 3DPSSM (40) and TITO (41).

NMR Spectroscopy—All of the NMR samples were prepared by dissolving the ^{15}N-labeled and unlabeled recombinant wheat ns-LTP2 in H_2O (10% D_2O), at a concentration of 2.8 mM in presence of 70 mM phosphate at pH 3.5 and 1 mM NaN_3. 1.5 eq of L-α-palmitoylphosphatidylglycerol (1-palmitoyl-2-Hydroxy-*sn*-glycero-3-[phospho-rac-(1-glycero)] sodium salt named LPG) was added to all of the protein preparations. Optimum phospholipid concentration was determined by a step by step titration monitored by ^{15}N HSQC. An improvement of the spectrum was observed with increasing lipid concentration from 0 to 1.2 eq, with further lipid addition having no effect on the protein spectrum. The NMR spectra were recorded on a Bruker AMX 600 spectrometer, operating at 599.94 MHz, equipped with a triple resonance inverse probe with a field gradient unit on the *z* axis. All of the data processing was performed with the version 4 of the *Gifa* software (42).

On the ^{15}N-labeled sample, a three-dimensional HSQC-TOCSY (45-ms mixing time, 80-h acquisition 305.2 K), a three-dimensional HSQC-NOESY (200-ms mixing time, 64-h acquisition 305.2 K), and a three-dimensional HSQC-NOESY (200-ms mixing time, 82-h acquisition, 295.2 K) were performed. Three-dimensional experiments were processed by linear prediction along the proton and ^{15}N indirect axes to obtain at least 256 complex points along each axis. Two two-dimen-

sional NOESY (200-ms mixing time, 18.5-h acquisition, 295.2 and 305.2 K) were also performed on this sample.

On the unlabeled sample, COSY, NOESY (200-ms mixing time), and TOCSY experiments were performed at the temperatures of 295.2, 310, and 323 K. Additional experiments were also performed in pure D_2O. Three NOESY experiments (τ_μ = 50, 100, and 200 ms) and a COSY experiment were performed on the unlabeled protein liganded with a perdeuterated dodecylphosphocholine lipid (DPC) as ligand and confirmed the assignment. Deuterium exchange experiments were performed by following the evolution of the TOCSY spectrum on a 3.3 mM sample in D_2O (60-ms mixing time, pH 3.3, 1 eq of LPG). To follow the most labile amide protons, the lyophilized protein was dissolved in D_2O at a temperature of 273 K. The exchange was then monitored by several experiments, slowly raising the temperature. The first spectrum was acquired at 273 K, starting directly after mixture, and a second one was acquired at the same temperature starting 3.5 h after the mixture. Then several spectra were acquired while raising the temperature to follow less labile protons: at 295.2 K 7 h after initial mixture and at 310 K 21 h after mixture. The sample was then left at room temperature for 4 days, and a final experiment was acquired at 295.2 K. A natural abundance ^{13}C HSQC experiment was performed in D_2O to confirm methylene assignment. Rotating frame NOE-edited spectroscopy experiments were performed at 295.2 K (50 and 100 ms) on the unlabeled protein liganded with LPG and with DPC. Diffusion ordered spectroscopy (43) was performed at 295.2 K (diffusion duration, 200 ms; gradient duration, 1.5 ms, with varying intensities from 0.5 to 47 G/cm, 1-h acquisition). Diffusion ordered spectroscopy experiments were performed on the unlabeled sample at 290 K, and the stimulated echo-longitudinal eddy current delay sequence (44, 45) was used with a WATERGATE filter applied for water suppression. A set of small monomeric globular proteins was measured under the same conditions to determine the molecular mass calibration.[2] Several ^{31}P NMR experiments were performed at 295.2 K on a AMX 400 Bruker spectrometer on a 2 mM sample (pH 3.5, 80 mM NaH_2PO_4 with 2.5 mM of LPG). Two ^{31}P exchange spectroscopy two-dimensional experiments (mixing time of 0.2 and 2 s, respectively) did not present any evidence of a bound/free equilibrium. All of the NMR data sets have been deposited in the NMRb data bank (nmrb.cbs.cnrs.fr; NMRb number ltpt2a).

NMR Spectra Assignment—The assignment of the wheat ns-LTP2 complexed with the phospholipid was performed from the set of three-dimensional (HSQC-NOESY and HSQC-TOCSY) and two-dimensional experiments (COSY, TOCSY, and NOESY) using the sequential assignment strategy (47) with the help of the Rescue software for the amino acid typing step (48). The assignment module of the *Gifa* program was used for this purpose (49).

In the HSQC experiment, all of the amide peaks could be found. All of the side chain labile hydrogens from Lys, Asn, Arg, and Gln residues were also assigned. Additional peaks belonging to the glycosylated proteins were sorted out in the HSQC spectrum from their reduced intensity. On the basis of sequential dNN(i,i+1) and dαN(i,i+1) all of the amino acids have been found, and 98% of all the nonlabile ^1H chemical shifts have been assigned. The natural abundance ^{13}C HSQC spectrum was used to help the assignment of side chain methylenes. Stereospecific assignment of β protons of methylene groups was performed by examination of the NOE intensity and coupling constant patterns.

Under the experimental conditions and because of the blurring of the NOE spectra caused by the exchange cross-peaks, the phospholipid signal could not be unambiguously assigned, except for the C16-terminal methyl protons. The complete assignment of the ^1H and ^{15}N chemical shifts of the wheat ns-LTP2 complexed with LPG has been deposited in the BioMagResBank (number 4977).

NMR Structure Calculation and Analysis—The two-dimensional and three-dimensional NOESY experiments, performed at three different temperatures (295.2, 310, and 323 K), have been used to extract all of the distance constraints used for the structure reconstruction. Peak intensities were calibrated against a set of reference peaks, using the standard tools provided with the *Gifa* program (49). Intensity levels were analyzed with a $1/r_6$ law, and distance constraints were obtained from the intensities by classifying in long, medium, and short range distances; pseudo-atom corrections were used. Additional constraints were obtained on the φ angle by measuring ^3J NH-Hα couplings constants using the Ludvigsen method (50) and on the χ_1 angle by considering the NOESY peak intensity between HN,Hα spins and Hβ_1,Hβ_2 spins, when a stereospecific assignment was available.

The dynamical annealing protocol (anneal.inp) of the crystallography NMR (CNS) software (51) was used to generate the protein structure from the set of constraints. A first set of structures was obtained from the constraint list, without any constraint on the cysteine linkage and with no phospholipid in the topology. From this set of structures, the disulfide linkage could be unambiguously assigned, because all of the sulfur atoms were located in compatible distances. The observed disulfide bridges are: Cys-25/Cys-60, Cys-10/Cys-24, Cys-2/Cys-34, and Cys-36/Cys-67. Hβ-Hβ NOE contacts were further observed in the NOESY map, which confirmed this assignment.

The model of the liganded protein was constructed from the same set of constraints. Additional constraints were used, corresponding to the observed connectivity of the C16 terminal CH3 of the fatty acid chain with Hδ and Hϵ of Tyr-44 and Tyr-47 and the middle of the lipidic chain (C8) with Hβ of Phe-35 with a long distance constraint. No additional constraint was used to force the exit of the phospholipid from the protein core. The distance constraints corresponding to the S-S bounds were then added to the constraint list. The dynamical annealing protocol was used for the calculation of 250 structures, from which the 10 structures with the lowest global energy were conserved. The obtained set of structures was deposited to the Protein Data Bank (code 1N89).

The Procheck (52) program was used to check the quality of the obtained structures, as well as to compute the Ramachandran maps. The Voidoo (53–55) was used to compute the volume of the inner cavity,

RESULTS AND DISCUSSION

Production and Purification—The recombinant protein preparations were obtained as previously described (34–36). The N-terminal sequence (ACQASQLAVC) of the recombinant ns-LTP2, determined by mass spectroscopy, is identical to those of the wheat-purified ns-LTP2 (56), indicating that the recombinant protein was correctly processed by the *P. pastoris* KEX2 protease.

The mass spectroscopy was performed on the ^{15}N-labeled protein. A 7055-Da average molecular mass was measured, confirming a ^{15}N isotopic labeling over 95%. The mass spectrum also revealed that approximately 15% of the protein has been glycosylated with one to four C6 sugar moieties, assumed to be mannose (162 Da). This is consistent with the fact that *P. pastoris* adds *O*-oligosaccharides composed solely of mannose residues. Peptide mass fingerprinting of the digested protein revealed that only the first tryptic fragment at the N terminus of the protein (fragment 1–29) is glycosylated.

N-Glycosylation requires the Asn-Xaa-Ser/Thr consensus sequence, whereas *O*-glycosylation requires the presence of a Ser or Thr residue. The wheat ns-LTP2 does not contain the Asn-Xaa-Ser/Thr sequence in its first 29 residues; however, it does contain four serine residues (at positions −5, 12, 16, and 21) and one threonine residue (at position 27), residues that are accessible for possible glycosylation. The presence of a proline residue in the vicinity of a serine or threonine residue can enhance *O*-mannosylation (57). Of the four serine residues available for *O*-linkage, residue 21 is the only one close to a proline residue. All of these results indicated that a small fraction of the wheat ns-LTP2 is expressed as a *O*-glycosylated protein. To our knowledge, no glycosylation has been reported for ns-LTP purified from plant.

Physicochemical Context Screening and Ligand Choice—Intensive screening of the physicochemical solution conditions was performed to find a set of conditions that provides NMR spectra of good quality. Ligand nature and ionic strength conditions were found to be critical.

Fluorescence screening experiments were performed on a series of phospholipids and fatty acids, highlighting a higher affinity for negatively charged phospholipids. We finally selected LPG with an average chain length (C16). The titration of ns-LTP2 by LPG, monitored by NMR, shows that the ns-LTP2 becomes more structurally constrained in the presence of this ligand. A narrowing and a spreading out of the peaks are observed on the two-dimensional HSQC spectrum. This evolu-

[2] P.-O. Schmidt, S. Augé, and M.-A. Delsuc, personal communication.

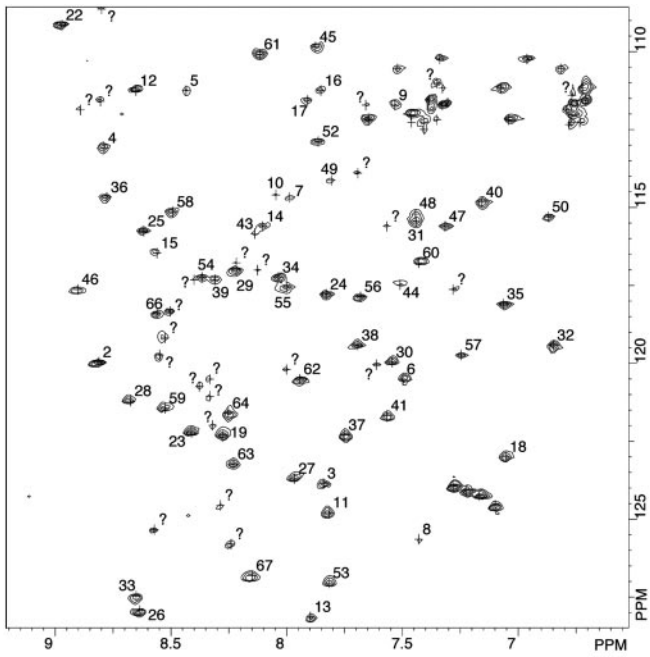

FIG. 2. **HSQC spectrum of ^{15}N-labeled recombinant wheat ns-LTP2.** The spectrum has been recorded at 295.2 K on a Bruker AMX 600 on a 2.8 mM sample complexed with 4.2 mM of L-α-palmitoylphosphatidylglycerol in 70 mM phosphate buffer at pH 3.5. The assignment is indicated by numbering the peaks with the identity of each residue. Unassigned peaks are indicated with *question marks*.

tion is stabilized around 1 eq of LPG. The addition of 70 mM phosphate buffer was observed to also improve spectral quality (Fig. 2). On the other hand, we found that the protein could adapt a large range of pH (3.45–6.5) and temperatures (273 K to 323 K) without important modification of the HSQC spectra.

Under these conditions, a diffusion ordered spectroscopy experiment was used to determine the translational diffusion coefficient of the protein in the experimental conditions, found at 117 μm2/s. Based on a calibration performed on a series of small globular proteins measured in the same conditions, this value confirms that the sample is monomeric. This result is in good agreement with the relaxation study, which has determined a rotational correlation time compatible with a monomeric form (58).

Under these optimized conditions, the ^{1}H-^{15}N HSQC spectrum of the ^{15}N-labeled ns-LTP2 protein liganded with LPG displays more peaks than expected, considering the number of residues. A second step of purification designed to remove the glycosylated proteins was performed on the sample, and a ^{1}H-^{15}N HSQC was recorded. This spectrum displays a reduced number of peaks, but the peaks are still too numerous (labeled with *question marks* in Fig. 2).

One-dimensional and exchange spectroscopy two-dimensional ^{31}P spectra were recorded on this sample. Two phosphorous lines can be observed in the one-dimensional spectrum, corresponding to the bound phospholipid and to the slight excess of free phospholipid in solution. No additional peaks nor any exchange peak could be observed in the exchange spectroscopy spectra, even at very long mixing time. To observe eventual chemical exchange, a two-dimensional ^{1}H rotating frame NOE-edited spectroscopy experiment was performed on the LPG-liganded protein. In this spectrum a strong exchange peak is visible in the Hα region, as well as several weaker peaks close to the diagonal in the aliphatic and amide regions. The same peaks are observed when the LPG ligand is replaced with a fully deuterated DPC phospholipid. An exchange between the holo and the apo states of the protein being excluded by the ^{31}P experiments, this is an indication that a conformational equilibrium between a major and a minor form of the protein is taking place. This equilibrium is the source of the additional peaks observed in the HSQC spectra. It was taken into account during the assignment phase, and several peaks were assigned to the minor form. However, no effort was done to fully assign this minor form.

Assignments and Secondary Structure Elements—The assignment of the protein resonances was performed from the set of ^{15}N-edited NOESY and TOCSY spectra. The sequential strategy was used, aided by the ^{15}N and natural abundance ^{13}C HSQC spectra (Fig. 3).

The solvent protection experiments indicate that the secondary structure is quite strongly established, because about 40% of the amide protons remain unexchanged during the first hours of the D_2O exchange experiment at 1 °C, and eight remain unexchanged after 5 days at room temperature. The solvent protection patterns, as well as J-coupling and NOESY patterns, are indicative of a structure mostly helical. On the other hand, the secondary structure prediction program Jpred (59) anticipates two helical zones, ranging from residues 22 to 29 and from residues 33 to 39.

Chemical assays as well as mass spectroscopy have shown that all eight cysteines of the protein are engaged in disulfide bridges. We have not been able to unambiguously assign the Hβ-Hβ NOE contacts characteristic of this structure because of the crowding of this spectral region. However, after the first run of structure generation, all of the obtained structures exhibited side chain proximities permitting the disulfide skeleton based on these prestructures to be assigned. The disulfide bridges thus found are: Cys-25/Cys-60, Cys-10/Cys-24, Cys-2/Cys-34, and Cys-36/Cys-67. This is in agreement with the chemically determined assignment (32).

The ^{1}H assignments of the LPG in the complexed form were obtained from two-dimensional COSY homonuclear experiments on the free LPG and by comparing the homonuclear spectra obtained from the LPG-ns-LTP2 complex and from the DPC-ns-LTP2 complex. A few chemical shifts of the fatty acid chain were clearly identified: the terminal methyl group (C16), its vicinal methylene (C15), as well as the proximal methylene (C2); the glycerol moiety attached to the fatty acid chains was also assigned. Some intermolecular NOE contacts were observed.

Structure Determination—From the complete set of geometric constraints extracted from the NMR spectra, a set of 10 structures has been obtained. They do not display any important constraint violation, and all of the residues are localized in the allowed regions of the Ramachandran plot. The ensemble of the10 best structures present a root mean square deviation computed on residues 2–67 of 0.9 Å for all of the heavy atoms and a root mean square deviation of 0.67 Å for the backbone atoms. All of the statistics of the geometrical constraints and the structure reconstruction are given in Table I. The set of solution structures of ns-LTP2 liganded with LPG as obtained from this experimental work is presented in Fig. 4.

The protein is observed as a globular protein with a diameter of about 30 Å. The structure is composed of five helices arranged in a superhelix tertiary structure. Helix 1 is a 3–10 helix, encompassing residues 7–15. All of the other helices are α-helices. Helix 2 includes residues 22–31, helix 3 includes residues 34–40, helix 4 includes residues 44–49, and helix 5 includes residues 51–60. The overall fold is a right superhelix. The localization of the helices is in good agreement with the proton exchange experiment, which has shown that there are five main zones in which the amide protons are protected against solvent exchange: residues 14 and 15, residues 26–31,

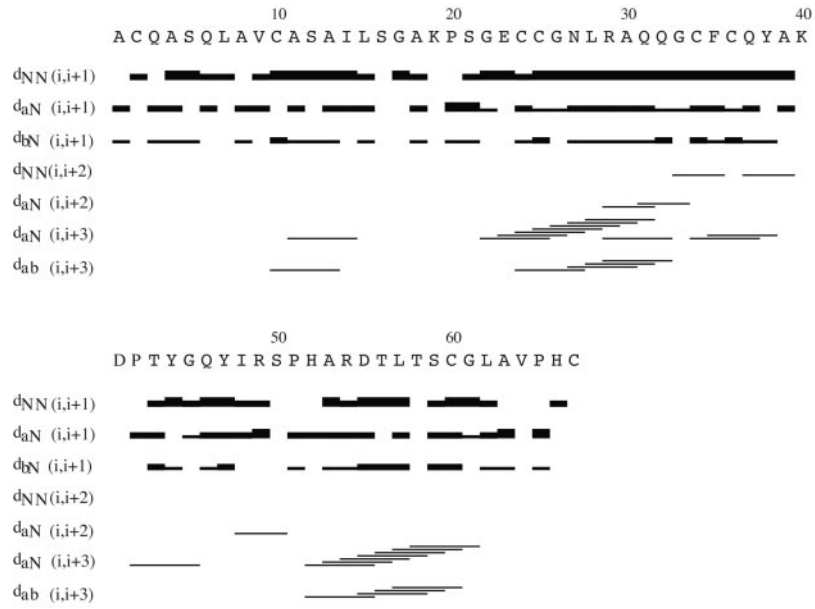

FIG. 3. **Synthetic plot showing the elements used for the structure determination.**

TABLE I
NMR restraints and structural statistics of the ensemble calculated for LPG-liganded wheat ns-LTP2 (10 structures)

Distance & angles restraints	
NOE intraresidual	403
NOE sequential (i, $i + 1$)	188
NOE medium range ($\|i - j\| \leq 3$)	72
NOE long range ($\|i - j\| > 3$)	95
NOE Intermolecular	5
S-S bridges	4
Dihedral angle ϕ	29
Dihedral angle χ_1	8
Total	800
Deviation from idealized geometry	
Bonds (Å)	0.00323 ± 0.00013
Angles	0.372 ± 0.012
Improper angles	0.187 ± 0.017
Dihedral angles	30.16 ± 3.04
Deviation from restrains	
NOE restrains	0.029 ± 0.001
Dihedral restrains	0.45 ± 0.1
Ramachandran plot (see Ref. 52)	
Most favored regions	74.2%
Allowed regions	23.5%
Generously allowed regions	2.4%
Disallowed regions	0.0%
Mean energies (kcal/mol)	
E_{bon}	10.29 ± 0.61
E_{ang}	37.14 ± 2.5
E_{imp}	2.67 ± 0.54
E_{vdw}	23.5 ± 3.8
E_{noe}	48.5 ± 3.93
E_{cdih}	0.94 ± 0.39
Root mean square deviation from average structure (Å) (residues 2–67)	
Backbone	0.67
Heavy atom	0.90

residues 38–41, residues 47–50, and residues 56–64. The LPG molecule is found partly embedded in the structure of the protein, with the superhelix structure of the protein coiled around the fatty acid chain, and with the phosphate group and the external glycerol moiety unstructured and located outside of the core of the protein.

Helices 1 and 2 are organized in a near anti-parallel conformation. The contact between helices 1 and 2 is tightened by the Cys-10/Cys-24 disulfide bridge. They are linked by an extended strand from Ser-16 to Gly-22. Lys-19 appears to be oriented toward the solvent and does not display any NOE contact with other residue. It should be noted that in a previous dynamic study, it has been observed that the H-N vector of Lys-19 is highly mobile in the ns range (58). Helices 3–5 form a square configuration. Helix 3 contains a characteristic Cys-34, Phe-35, Cys-36 pattern, with Phe-35 buried into the structure and contributing to the hydrophobic core of the structure. Cys-34 and Cys-36 are respectively engaged in disulfide bridges with Cys-2 and Cys-67, forming two diametrically opposed bonds relative to the helix axis. All of the prolines are observed in trans conformation, as confirmed by the H$\alpha(i)$–Hδ-Pro(i + 1) contacts observed in the NOESY spectra, for all of the proline residues (Pro-20, Pro-42, Pro-51, and Pro-65).

Several additional secondary structure elements can be observed in the structure. The C-terminal of helix 1 presents an unusual hydrogen bond pattern, with the carboxyl moiety of Ser-12 being engaged with the HN of Ala-18. This structure is found in the 10 structures generated, and the HN of residue Ala-18 is found to be protected against solvent exchange, thus confirming this result. A type-1 γ turn is observed between helices 2 and 3, corresponding to residues Gln-31, Gln-32, and Gly-33. A type-1 β turn is observed between helices 3 and 4, corresponding to residues Asp-41, Pro-42, Thr-43, and Tyr-44, with the acidic head of Asp-41 engaged in a hydrogen bond with the HN of Thr-43. Three classic helix cappings can also be observed: the N-capping of helix 2 with the OH of Ser-21 hydrogen-bonded to the HN of Glu-23; the C-capping of helix 2 with the side chain of Gln-32 bonded to the CO of Arg-29; and the N-capping of helix 5, with the OH of Ser-50 bonded to the HN of His-52. Finally, a transient slat bridge between the amide moiety of Lys-40 and the C terminus of the backbone can be observed in several structures of the NMR ensemble.

The protein presents an inner cavity, which has been measured at 341 Å^3. All of the helices present hydrophobic side chains directed toward the cavity. The phospholipid is found in this cavity. Only one unique phospholipid position is observed in the cavity for all 10 retained structures. The fatty acid chain is completely embedded in the protein structure. Its axis is aligned with the axis of the tertiary superhelix and is orthogonal to the α-helix axes (Fig. 4*c*). The terminal methyl group is positioned between the H1 and H4 helices. The fatty acid chain is inserted in the cavity constituted by the hydrophobic residues (Leu-7, Leu-28, Phe-35, Tyr-38, Tyr-44, Tyr-47, Ile-48, Ala-53, Leu-57, Val-64, and Pro-65). The chain presents a turn near carbon 8 and exits the cavity in a cleft between helices H4 and H5 and the C-terminal residue. The inner glycerol moiety

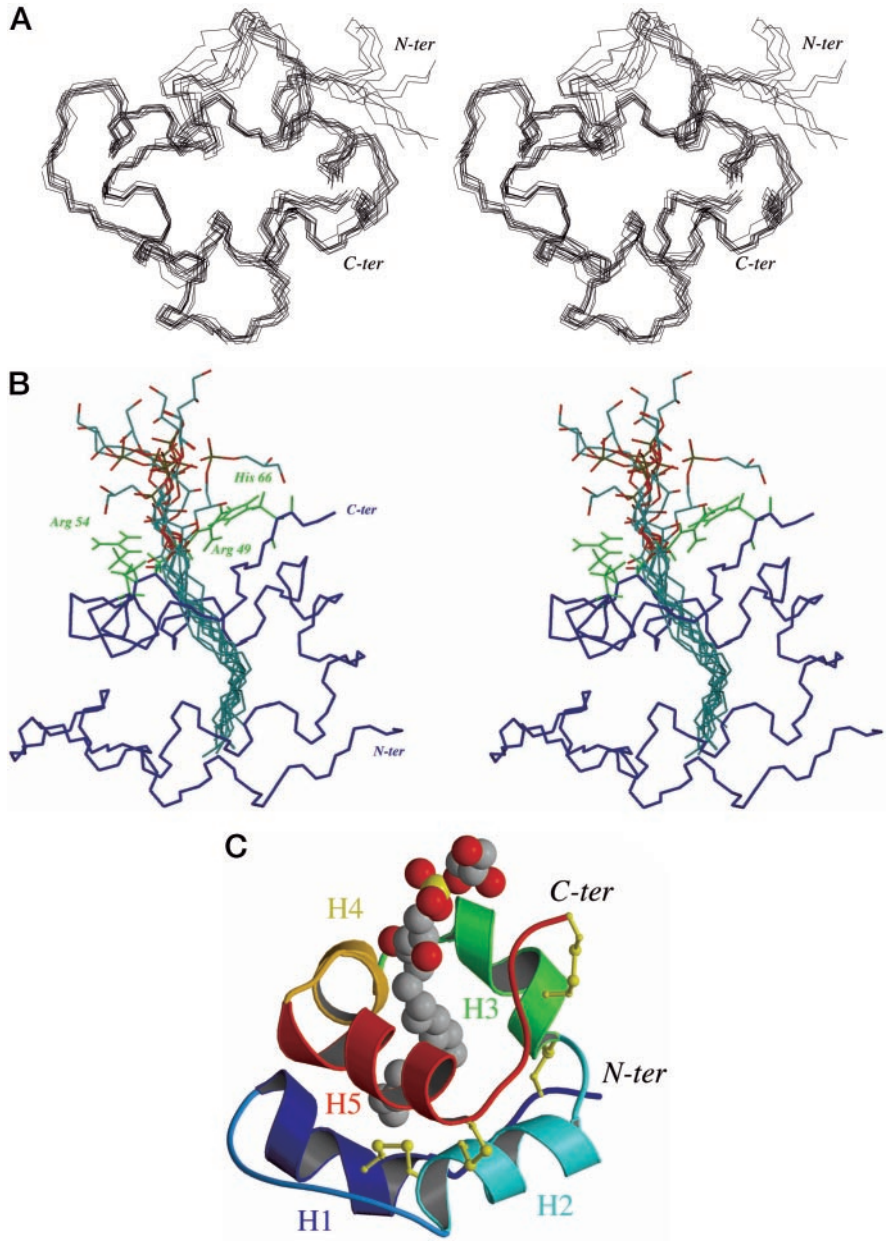

FIG. 4. *a*, stereo view of the best 10 NMR structures of wheat ns-LTP2. The phospholipid is not shown for clarity. *b*, mean NMR structure, with the ensemble of the phospholipid structure as observed in the 10 best protein generated structures. The orientation is rotated by 90° along the OX axis with respect to *panel a*. Basic residues around the phosphate group are marked in *green*. *c*, schematic view of the structure of ns-LTP2 with a CPK model of the liganded phospholipid. The orientation is the same as in *panel b*.

is located on a pocket on the surface of the protein. This pocket presents a basic environment constituted by the Arg-49, Arg-54, and His-66 side chains. These basic residues are observed in close proximity with the phosphate moiety, equilibrating the phosphate charge (Fig. 5). The cavity of ns-LTP2 is asymmetric. The proximal entrance of the cavity, where the phosphate group is found, presents several hydrophilic and basic groups: Arg-49, Arg-54, Thr-58, and His 66. The distal opening of the cavity is characterized with hydrophobic residues, such as Leu-7, Tyr-38, Tyr-44, and Tyr-47.

This location is in good agreement with the following spectroscopic observations: In the fatty acid chain only three unambiguous NOE intermolecular contacts have been identified. Four NOE contacts connect the LPG-terminal methyl groups (C16) with the Tyr-44 and Tyr-47 aromatic part. The other NOE connects the one of the methylenes of the fatty acid chain with the Hβ of Phe-35. All of these residues are found in the hydrophobic cavity. No NOE contacts were found between the protein and LPG glycerol moiety. The chemical shifts of the phospholipid glycerol moiety do not present much shift upon complexation with the protein. On the other hand, the fatty acyl chain chemical shift differences between isolated and liganded LPG are important.

The structure of the minor form present in solution has not been studied, even though it appears to be structured. About one-third of the amino acids seem to be involved in the conformation equilibrium; no attempt was made to assign the residues involved in this equilibrium. Previous dynamic study (58) has shown that the major form is predominantly rigid, with S^2 ranging from 0.8 to 0.9, except for Lys-19, exposed to the solvent.

ns-LTP2 versus ns-LTP1 Comparison—The three-dimensional structure is known for several ns-LTP1 from different species (19–29). They are very similar among plant and consist in four α-helices organized in a superhelix structure and connected by four disulfide bridges. We compared the structure we present here with wheat ns-LTP1 (Protein Data Bank code 1gh1) (19) using the Visual Molecular Dynamics software (46) (Fig. 6).

The best superposition is obtained when the H1, H2, and H5 (residues 3–16, 22–32, and 50–63) helices in ns-LTP2 are superimposed with the H1, H2, and H4 helices (residues 5–8,10–

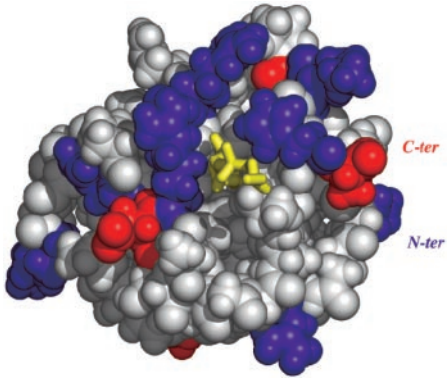

FIG. 5. **CPK representation of the ns-LTP2 structure.** Positively charged residues are colored *blue* and negatively charged residues are colored *red*; the phospholipid is represented in licorice mode. It can be seen how the terminal glycerol group sticks out of the molecular surface and how the basic residues surround the phosphate group (in *yellow*). The orientation is similar to that in Fig. 4*a*.

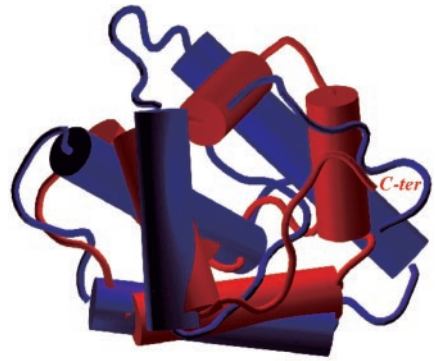

FIG. 6. **Structural comparison of wheat ns-LTP2 (*red*) with wheat ns-LTP1 (Protein Data Bank code 1gh1) (*blue*).** Orientation is the same as in Fig. 4*a*, only ns-LTP2 C-terminal and N-terminal are labeled. Superposition of helices 1, 2, and 5 (ns-LPT2 numbering) with equivalent helices in ns-LTP1 can clearly been observed. Helices 3 and 4 with no equivalent in ns-LTP1 are also observed in front.

19, 23–35, and 63–76) in ns-LTP1. This gives a root mean square deviation of 1.88 Å (backbone only). The global structure is similar and consists in an hydrophobic cavity structure adapted to the lipid transport. Nevertheless, large three-dimensional structural differences between ns-LTP1 and ns-LTP2 are observed in two regions: the H3 and H4 (respectively H3) α-helices and the C-terminal region. The last turn of the H2 helix is also different in both structures.

The two short H3 and H4 α-helices orthogonal to each other in ns-LTP2 are replaced by the longer H3 helix in ns-LTP1. ns-LTP1 H3 helix is oriented differently and flanked by two large loops presenting no regular secondary structure. This structural difference opens up the cleft corresponding to the entrance of the cavity in which the ligand is located. The C terminus of ns-LTP1 presents a large loop with no secondary structure. The corresponding zone is deleted in ns-LTP2, thus releasing access to the hydrophobic cavity. This deletion has globally no impact on the position of the disulfide bridge involving the last cysteine (Cys-67), which is conserved. As a consequence of these structural changes, the wheat ns-LTP2 is smaller and more globular than ns-LTP1.

All of the cysteine residues are involved in disulfide bridges, but the wheat ns-LTP2 differs from ns-LTP1 in the way the connections are made between the cysteines. ns-LTP1s exhibit a conserved CXC motif located in helix 3, with X being an hydrophilic residue. The two cysteines flanking this hydrophilic residue are linked to cysteines at distal positions in a crossed scheme (as showed in Fig. 1). In the wheat ns-LTP2, an hydrophobic residue (Phe-35) is present, and the two flanking cysteines are involved in disulfide bridges in a noncrossed scheme. The hydrophobic side chain of Phe-35 is displayed on the cavity surface of the wheat ns-LTP2, whereas in ns-LTP1 the corresponding hydrophilic residue is exposed to the solvent, because of a 180° rotation of the entire helix 3 along its main axis.

This cysteine linkage pattern is not unique to ns-LTP2 and is observed in the soy bean hydrophobic protein. Searching structural data bases (40) for a protein presenting a similar structural arrangement to ns-LTP2, the soy bean hydrophobic protein (Protein Data Bank code 1hyp) is found as the best match. This protein shares some structural similarity with ns-LTPs but does not transfer lipids. It presents an analogous organization in terms of helix number and orientation, as well as disulfide bridge topology. Helix 3 is involved in a noncrossed disulfide bridge scheme and appears not to be amphiphilic when compared with ns-LTP2. This could explain why soy bean hydrophobic protein does not exhibit lipid transfer capability.

The presence of an hydrophobic cavity is a characteristic of ns-LTPs; the hydrophobic ligands are bound in this cavity in a rather nonspecific manner. No major differences have been observed between the structure of the free and palmitate complexed maize (21) and barley (25) ns-LTP1 and free and prostaglandin B2-liganded wheat ns-LTP1 (29), whereas large conformational changes have been seen for barley ns-LTP1 when it complexes with palmitoyl CoA (25). Orientation of the lipid within the hydrophobic cavity was found to be opposite in maize (21) and barley (26) liganded structures, whereas wheat ns-LTP1 is able to bind two monoacylated lipids insert head to tail in the hydrophobic cavity (28).

Measured volumes of this hydrophobic cavity are highly variable in ns-LTP1 (23), with typical values ranging from 150 to 580 $Å^3$. However, barley ns-LTP1 exhibits a large volume change upon palmitoyl-CoA binding, with a measured cavity volume increasing from 39 to 620 $Å^3$. The volume observed for the wheat ns-LTP2 appears to be in the same range, even though the protein is smaller by 24 amino acids.

The orientation of the phospholipid main chain, observed in ns-LTP2, is roughly orthogonal to the α-helix axes, and the chain runs from helices H1 to H5. This is in contrast with most described ns-LTP1 cavities found with a main axis parallel to the α-helix axes.

Conclusion—The present work presents the refined structure of the wheat ns-LTP2 protein, liganded with L-α-palmitoylphosphatidylglycerol, as determined by NMR spectroscopy. The protein was observed as being composed of five helices, structured as a right superhelix, surrounding the phospholipid. This structure presents some homologies with other lipid transfer proteins such as ns-LTP1; however, the phospholipid was found in a quite different location than in most LTP1s. An hydrophobic cavity was also observed, with a volume equivalent to the one found in ns-LTP1 but with a different geometry.

The ns-LTP2 protein structure also presents homology with the one soy bean hydrophobic protein that does not exhibit any lipid transfer activity. This permits us to devise a protein family encompassing ns-LTP1 and ns-LTP2 but also soy bean hydrophobic protein and other related vegetal proteins, based on structural homologies, rather than on the function of primary sequence homologies.

Extensive ligand screening had to be undertaken to find a set of conditions allowing structural study. This indicates that even if the ns-LTP2 is able to adapt a large number of hydrophobic ligands in its hydrophobic pocket, it certainly presents varying affinities depending on the nature of the ligand. The better affinity for single chain phospholipid, negatively charged,

can be explained *a posteriori*, by the size of the pocket and by the patch of positively charged residues located around its entrance. Further comparative studies on this protein and on homologous proteins will have to be undertaken to improve the understanding on the phospholipid binding affinity and of the phospholipid transfer activity.

Finally it remains to be explained how the structural differences observed in the plant LTP family might be related to the various *in vivo* activities putatively assigned to its members. Comparative structural and dynamical studies on several isoforms of wheat ns-LTPs are currently in progress in our group. This complementary work should permit us to draw stronger links between structural features and biological functions.

Acknowledgments—We acknowledge N. Sommerer for mass spectrometry analysis; C. Royer, C. Blanchard, and F. Vagner for helping in the fluorescence and HSQC screening experiments; and the VMD team for efficient support.

REFERENCES

1. Kader, J. C., Julienne, M., and Vergnolle, C. (1984) *Eur. J. Biochem.* **139,** 411–416
2. Kader, J. C. (1996) *Annu. Rev. Plant Physiol. Plant Mol. Biol.* **47,** 627–654
3. Kader, J. C. (1997) *Trends Plant Sci.* **2,** 66–70
4. Sterk, P., Booij, H., Schellekens, G., Kammen, A. V., and Vrie, S. C. D. (1991) *Plant Cell* **3,** 907–921
5. Hendriks, T., Meijer, E. A., Thoma, S., Kader, J. C., and De Vries, S. C. (1994) in *Plant Molecular Biology* (Corruzi, G., and Puigdomenech, G. P., eds) Vol. H81, pp. 85–94, Springer Verlag, Berlin
6. Terras, F. R. G., Goderis, I. J., Leuven, F. v., Vanderleyden, J., Cammue, B. P. A., and Broekaert, W. F. (1992) *Plant Physiol.* **100,** 1055–1058
7. Garcia-Olmedo, F., Molina, A., Segura, A., and Moreno, M. (1995) *Trends Microbiol.* **3,** 72–74
8. Blein, J. P., Coutos-Thevenot, P., Marion, D., and Ponchet, M. (2002) *Trends Plant Sci.* **7,** 293–296
9. Demura, T., and Fukuda, H. (1993) *Plant Physiol.* **103,** 815–821
10. Ye, Z. H., and Varner, J. E. (1994) *Proc. Natl. Acad. Sci. U. S. A.* **91,** 6539–6543
11. Jakobsen, K., Sletner, S., Aalen, R. B., Bosnes, M., Alexander, D., and Olsen, O. A. (1989) *Plant Mol. Biol.* **12,** 285–293
12. Garcia-Garrido, J. M., Menossi, M., Puig-Domenech, P., Martinez-Izquierdo, J. A., and Delseny, M. (1998) *FEBS Lett.* **428,** 193–199
13. Krause, A., Sigrist, C., Dehning, L., Sommer, H., and Broughton, W. (1994) *Mol. Plant Microbe Interact.* **7,** 411–418
14. Sánchez-Monge, R., Lombardero, M., García-Sellés, F. J., Barber, D., and Salcedo, G. (1999) *J. Allergy Clin. Immunol.* **103,** 514–519
15. Pastorello, E. A., Pompei, C., Pravettoni, V., Brenna, O., Farioli, L., Trambaioli, C., and Conti, A. (2001) *Allergy* **5,** 45–47
16. Pastorello, E. A., Pravettoni, V., Farioli, L., Ispano, M., Fortunato, D., Monza, M., Giuffrida, M. G., Rivolta, F., Scibola, E., Ansaloni, R., Incorvaia, C., Conti, A., and Ortolani, C. (1999) *J. Allergy Clin. Immunol.* **104,** 1099–1106
17. Asero, R., Mistrello, G., Roncarolo, D., de Vries, S. C., Gautier, M. F., Ciurana, C. L. F., Verbeek, E., Mohammadi, T., Knul-Brettlova, V., Akkerdaas, J. H., Bulder, I., Aalberse, R. C., and van Ree, R. (2000) *Int. Arch. Allergy Immunol.* **122,** 20–32
18. Toriyama, K., Hanaoka, K., Okada, T., and Watanabe, M. (1998) *FEBS Lett.* **424,** 234–238
19. Gincel, E., Simorre, J. P., Caille, A., Marion, D., Ptak, M., and Vovelle, F. (1994) *Eur J Biochem.* **226,** 413–422
20. Heinemann, B., Andersen, K. V., Nielsen, P. R., Bech, L. M., and Poulsen, F. M. (1996) *Protein Sci.* **5,** 13–23
21. Shin, D. H., Lee, J. Y., Hwang, K. Y., Kim, K. K., and Suh, S. W. (1995) *Structure* **3,** 189–199
22. Gomar, J., Petit, M. C., Sodano, P., Sy, D., Marion, D., Kader, J. C., Vovelle, F., and Ptak, M. (1996) *Protein Sci.* **5,** 565–577
23. Lee, J. Y., Min, K., Cha, H., Shin, D. H., Hwang, K. Y., and Suh, S. W. (1998) *J. Mol. Biol.* **276,** 437–448
24. Poznanski, J., Sodano, P., Suh, S. W., Lee, J. Y., Ptak, M., and Vovelle, F. (1999) *Eur. J. Biochem.* **259,** 692–708
25. Lerche, M. H., Kragelund, B. B., Bech, L. M., and Poulsen, F. M. (1997) *Structure* **5,** 291–306
26. Lerche, M. H., and Poulsen, F. M. (1998) *Protein Sci.* **7,** 2490–2498
27. Sodano, P., Caille, A., Sy, D., de Person, G., Marion, D., and Ptak, M. (1997) *FEBS Lett.* **416,** 130–134
28. Charvolin, D., Douliez, J., Marion, D., Cohen-Addad, C., and Pebay-Peyroula, E. (1999) *Eur. J. Biochem.* **264,** 562–568
29. Tassin-Moindrot, S., Caille, A., Douliez, J.-P., Marion, D., and Vovelle, F. (2000) *Eur. J. Biochem.* **267,** 1117–1124
30. Tassin, S., Broekaert, W. F., Marion, D., Acland, D. P., Ptak, M., Vovelle, F., and Sodano, P. (1998) *Biochemistry* **37,** 3623–3637
31. Monnet, F.-P. (1990) *Characterization of a Hard Wheat Lipid Binding Protein. Purification, Sequencing and cDNA Cloning.* Ph.D. thesis, Université des Sciences et Techniques du Languedoc, Montpellier, France
32. Douliez, J.-P., Pato, C., Rabesona, H., Mollé, D., and Marion, D. (2001) *Eur. J. Biochem.* **268,** 1400–1403
33. Dharmaraj, S., Yaw-Jen, L., Chao-Sheng, C., and Ping-Chiang, L. (2002) *J. Biol. Chem.* **277,** 35267–35273
34. de Lamotte, F., Boze, H., Blanchard, C., Klein, C., Moulin, G., Gautier, M.-F., and Delsuc, M.-A. (2001) *Protein Expression Purif.* **22,** 318–324
35. Klein, C., de Lamotte-Guery, F., Gautier, F., Moulin, G., Boze, H., Joudrier, P., and Gautier, M. F. (1998) *Protein Expression Purif.* **13,** 73–82
36. de Lamotte, F., Klein, C., Issaly, N., Gautier, M.-F., and Boze, H. (1999) *Biotechnol. Techniques* **13,** 351–354
37. Higgins, D., Thompson, J., Gibson, T., Thompson, J. D., Higgins, D. G., and Gibson, T. J. (1994) *Nucleic Acids Res.* **22,** 4673–4680
38. Altschul, S., Madden, T., Schaffer, A., Zhang, J., Zhang, Z., Miller, W., and Lipman, D. (1997) *Nucleic Acids Res.* **25,** 3389–3402
39. Douguet, D., and Labesse, G. (2001) *Bioinformatics* **17,** 752–753
40. Kelley, L. A., MacCallum, R. M., and Sternberg, M. J. E. (2000) *J. Mol. Biol.* **299,** 501–522
41. Labesse, G., and Mornon, J. (1998) *Bioinformatics* **14,** 206–211
42. Pons, J. L., Malliavin, T. E., and Delsuc, M. A. (1996) *J. Biomol. NMR* **8,** 445–452
43. Johnson, J. C. S. (1999) *Prog. Nuclear Magn. Reson. Spectroscopy* **34,** 203–256
44. Gibbs, S. J., and Johnson, C. S., Jr. (1991) *J. Magn. Reson.* **93,** 395–402
45. Wu, D. H., Chen, A. D., and Johnson, C. S. (1995) *J. Magn. Reson. Ser. A* **115,** 260–264
46. Humphrey, W., Dalke, A., and Schulten, K. (1996) *J. Mol. Graphics* **14,** 33–38
47. Wüthrich, K. (1986) *NMR of Proteins and Nucleic Acids*, pp. 117–161, John Wiley & Sons, Inc., New York
48. Pons, J. L., and Delsuc, M.-A. (1999) *J. Biomol. NMR* **15,** 15–26
49. Malliavin, T. E., Pons, J. L., and Delsuc, M. A. (1998) *Bioinformatics* **14,** 624–631
50. Ludvigsen, S., Andersen, K. V., and Poulsen, F. M. (1991) *J. Mol. Biol.* **217,** 731–736
51. Brunger, A. T., Adams, P. D., Clore, G. M., DeLano, W. L., Gros, P., Grosse-Kunstleve, R. W., Jiang, J. S., Kuszewski, J., Nilges, M., Pannu, N. S., Read, R. J., Rice, L. M., Simonson, T., and Warren, G. L. (1998) *Acta Crystallogr. Sect. D Biol. Crystallogr.* **54,** 905–921
52. Laskowski, R. A., Rullmann, J. A. C., MacArthur, M. W., Kaptein, R., and Thornton, J. M. (1996) *J. Biomol. NMR* **8,** 477–486
53. Kleywegt, G. J., and Jones, T. A. (1993) *CCP4/ESF-EACBM Newsletter on Protein Crystallography* **29,** 26–28
54. Kleywegt, G. J., and Jones, T. A. (1994) *Acta Crystallogr. Sect. D Biol. Crystallogr.* **50,** 178–185
55. Kleywegt, G. J., Zou, J. Y., Kjeldgaard, M., and Jones, T. A. (2001) in *Crystallography of Biological Macromolecules* (Rossmann, M. G., and Arnold, E., eds) Vol. F, pp. 353–356 and 366–367, Kluwer Academic Publishers, Dordrecht, The Netherlands
56. Monnet, F. P., Dieryck, W., Boutrot, F., Joudrier, P., and Gautier, M. F. (2001) *Plant Sci.* **161,** 747–755
57. Tanner, W., and Lehle, L. (1987) *Biochim. Biophys. Acta* **906,** 81–99
58. de Lamotte, F., Vagner, F., Pons, J.-L., Gautier, M.-F., and Delsuc, M.-A. (2001) *C. R. Acad. Sci. (Paris)* **4,** 839–843
59. Cuff, J. A., Clamp, M. E., Siddiqui, A. S., Finlay, M., and Barton, G. J. (1998) *Bioinformatics* **14,** 892–893